Passivity-based control of energy storage units in Distributed Generation Systems

Ricardo R. Peña *†, Roberto D. Fernández*†, Ricardo J. Mantz‡§ and Pedro E. Battaiotto ‡
*Laboratorio de Electrónica, Facultad de Ingeniería, Universidad Nacional de la Patagonia San Juan Bosco, Argentina.
Email: ramirop@unpata.edu.ar
†Consejo Nacional de Investigaciones Científicas y Tecnológicas CONICET, Argentina.
‡Facultad de Ingeniería, Universidad Nacional de La Plata, La Plata, Argentina.
§Comisión de Investigaciones Científicas de la Provincia de Buenos Aires, Argentina.

***Abstract*—Distributed generation systems (DGS) has become a promising alternative to meet the growing demand for electricity. The requirements for DGS systems justify the use of new control techniques that ensure stability and can handle the performance of the system. In this sense, passivity based control is a technique that takes advantage of the structure of the system by providing a better understanding of the control law. The main objective of this paper is to evaluate Power Shaping control to regulate active and reactive powers of an energy storage system in order to improve the performance of the electrical grid.**

***Index Terms*—Distributed generation systems, power shaping control, passivity-based control, Energy Storage Systems, sliding mode reference conditioning.**

I. Introduction

Distributed generation systems (DGS) offer advantages in terms of quality and availability of electricity supply. These systems are composed of multiple power generation units, renewable and non-renewable, interacting among them with nonlinear behaviors [1].

The capacity installed of renewable energy conversion systems for the production of electrical power has grown in recent decades. Thus wind energy and solar are positioned as the two most important renewable resources because this can be easily captured in contrast with other renewable resources [2], [3]. Particularly, the adoption of wind energy conversion systems (WECS), in the production of electric eenergy, reduces dependence on fossil fuels and pollution. Different WECS have been developed in order to increase system efficiency and with fault ride through capability [4].

In recent decades the integration of energy storage systems in electric power systems has been increasing gradually. The incorporation of energy storage systems (ESS) damps disturbances originated in the load or in the renewable generation units increasing the efficiency of the power generation system [5], [6], [3].

Some DGS problems have been addressed by linearization techniques [7], [6]. However the complexity of the DGS systems usually requires more advanced control techniques. In this sense, the work proposes the use of a nonlinear control technique based on Power Shaping (PS) control that ensures stability in a domain of attraction.

PS control, which is based on passivity ideas, was proposed in the paper [8]. PS control, uses a system description based on the equations of Brayton-Moser (BM). BM equations represents the dynamics of an electrical circuits in terms of current and voltages. These amounts can be measured without difficulty which facilitates construction of a controller as opposed to other techniques that uses charges and fluxes to model a system [9].

Power shaping control can be used to stabilize a nonzero equilibrium point, in this case, the storage function can be modified to achieve a minimum at this point [10].

In particular, we propose a control law for the ESS through Power Shaping control in order to control the active and reactive powers that the device can supply at the connection point.

Restrictions on the active and reactive powers that the ESS can deliver to the grid are considered in this paper. Particularly, a scheme that uses sliding mode reference conditioning technique (SMRC) is applied considering the maximum powers that the ESS can deliver to the grid.

The structure of this paper is as follows. Section II presents the dynamical model of the system analyzed. Section III introduces the power shaping ideas to design a controller for active and reactive power. The controller is evaluated in section IV. Finally, the conclusions are summarized.

II. System model

The system considered is shown in Fig. 1. This consists of a synchronous generator coupled with a diesel engine (GS_1), a distribution line (Z_1), a wind turbine (GA_1), an energy storage system (ESS) and a dynamic load based on induction motors connected to bus 1.

Generally, active and reactive powers in an node of the electrical grid are written in function of the voltage magnitude (V) and the angle (θ) of all nodes as

$$P_{nk} = V_k \sum_{m=1}^{n} (G_{km} V_m cos(\theta_{km}) + B_{km} V_m sin(\theta_{km})), \quad (1)$$

$$Q_{nk} = V_k \sum_{m=1}^{n} (G_{km} V_m sin(\theta_{km}) - B_{km} V_m cos(\theta_{km})), \quad (2)$$

where V_k is the voltage in the generic node k, G_k and B_k are the conductance and susceptance respectively, $\theta_{km} = \theta_k - \theta_m$ [11], [12].

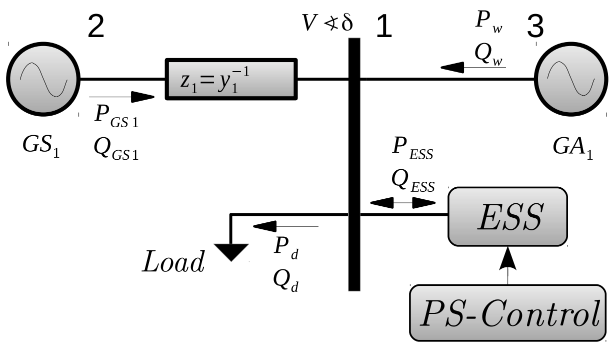

Figure 1. System analyzed.

The active and reactive powers balances at the node 1 (Fig. 1) are

$$P_{n1} = P_d - P_w \pm P_{ESS}, \tag{3}$$

$$Q_{n1} = Q_d - Q_w \pm Q_{ESS}, \tag{4}$$

where P_d, Q_d, P_w, Q_w, P_{ESS}, Q_{ESS} are the active and reactive powers consumed by the dynamic load, provided by the wind turbine and exchanged by the ESS with the electrical grid respectively (see Fig. 1).

A. Synchronous generator

The expressions that represent the dynamic behavior of a synchronous generator and the voltage controller, assuming that supplied torque by the prime mover and the flux are constant, become

$$\dot{\delta_1} = \omega_1 - \omega_r, \tag{5}$$

$$M_1\dot{\omega_1} + D_1\omega_1 = P_m - P_e, \tag{6}$$

$$T_A d\dot{E}_{fdi} = -E_{fdi} + K_a(V_{ref} - V), \tag{7}$$

with ω_1 the rotor angular velocity, ω_r is the line reference frequency, M_1 the inertia constant, D_1 is the internal friction of the machine, P_m is the power supplied by the prime mover and P_e is the electrical power. In the expression (7), E_{fdi} is field voltage, V_{ref} is the reference of voltage, V is the voltage at the terminals of the electrical machine, K_a and T_a are constants [11], [13].

B. Wind Turbine

The wind turbine considered in this work is basically composed of a horizontal axis rotor, a doubly-fed induction generator (DFIG) and a back to back converter. The wind turbine is modeled as a concentrated mass system. As a first approach to the problem, we consider that the wind speed is constant. Then, the active power injected by the wind turbine is constant. Furthermore, it is operated neutral to the grid i.e., ($Q_w = 0$ VAr).

C. Energy Storage System (ESS)

As stated above, the control actions are applied to the ESS. Which operates on the premise of providing power in cases of rapid fluctuations in load or variations in wind resource. The ESS must operate in the ranges of a few seconds, in this regard, the use of supercapacitors or flywheel technology is suitable [5]. Furthermore, the dynamics of ESS is so fast, that it is considered as a source of instantaneous power.

D. Dynamic load

The load includes a constant PQ and an induction motor loads

$$P_d = P_0 + P_1 + k_{pw}\dot{\delta} + k_{pv}(V + T\dot{V}), \tag{8}$$

$$Q_d = Q_0 + Q_1 + k_{qw}\dot{\delta} + k_{qv}V + k_{qv2}V^2, \tag{9}$$

where P_0 and Q_0 are the active and reactive constant powers, P_1 and Q_1 represent the PQ load, V is the voltage in the connection point and $\dot{\delta}$ is the frequency [14].

From the equation (4) is possible to obtain

$$\dot{\delta} = (Q_A - Q_0 - Q_1 - k_{qv}V - k_{qv2}V^2)/k_{qw}, \tag{10}$$

with $Q_A = Q_{n1} + Q_w \pm Q_{ESS}$, replacing in the expression (3), we have

$$\dot{V} = (P_A - P_0 - P_1 - k_{pw}\dot{\delta} - k_{pv}V)/(k_{pv}T), \tag{11}$$

with $P_A = P_{n1} + P_w \pm P_{ESS}$.

The load parameter used in this work are presented in the appendix A.

E. Mathematical model

The dynamical model of the system is given by

$$\begin{cases} \dot{x} = f(x) + g(x)u \\ y = h(x) \end{cases}, \tag{12}$$

where $x \in \mathbb{R}^n$ is the state vector and $x^T = \begin{bmatrix}\omega_1 & E_{fdi} & \delta & V\end{bmatrix}$, $u \in \mathbb{R}^m$ is the input vector with $m \leq n$, $f(x) : \mathbb{R}^n \to \mathbb{R}^n$ and $g(x) : \mathbb{R}^n \to \mathbb{R}^nx\mathbb{R}^m$. The equations which constitutes $f(x)$ are the dynamic load and the synchronous generator. The order of the system can be reduced if we introduce the relative angles in the synchronous generator [11]. Then, the expression (5) will not be included in the system model

$$f(x) = \begin{bmatrix} f_1(x) \\ f_2(x) \\ f_3(x) \\ f_4(x) \end{bmatrix}, \tag{13}$$

with:

$$\begin{aligned} f_1(x) &= \frac{(P_m - P_e - D_1x_1)}{M_1}, \\ f_2(x) &= \frac{(-x_2 + K_a(V_{ref} - V))}{T_a}, \\ f_3(x) &= \frac{(Q_A - Q_0 - Q_1 - k_{qv}x_4 - k_{qv2}x_4^2)}{k_{qw}}, \\ f_4(x) &= \frac{(P_A - P_0 - P_1 - k_{pw}\dot{x_3} - k_{pv}x_4)}{(k_{pv}T)}. \end{aligned} \tag{14}$$

The vector $g(x)$ is given by

$$g(x) = \begin{bmatrix} 0 & 0 \\ 0 & 0 \\ \frac{1}{k_{qw}} & 0 \\ 0 & \frac{1}{(k_{pv}T)} \end{bmatrix}. \tag{15}$$

III. Control design

In this section we summarize the main Power Shaping stabilization ideas. These ideas are used for proposing a controller by Power Shaping for the system described in the previous section.

A. Power Shaping Stabilization

The system (12) can be described employing the Brayton-Moser equations [9]

$$Q(x)\dot{x} = \frac{\partial P(x)}{\partial x} + g(x)u, \tag{16}$$

where $Q(x)$ is a full rank matrix, nonsingular and $P(x)$ is a mixed-potential function. In order to establish a control law by power shaping the next propositions are assumed according to [9] and [10]:

1) There exist a full range matrix $Q : \mathbb{R}^n \to \mathbb{R}^{nxn}$, non singular that solves the differential equation:

$$\nabla(Q(x)f(x)) = [\nabla(Q(x)f(x))]^T, \tag{17}$$

and furthermore verifies that:

$$Q(x) + Q(x)^T \leq 0. \tag{18}$$

2) There is a scalar function $P_a : \mathbb{R}^n \to \mathbb{R}$, positive definite in the neighborhood of an equilibrium point x^*, which verifies the following partial differential equation (PDE):

$$g^{\perp}(x)Q^{-1}(x)\nabla P_a(x) = 0, \tag{19}$$

where $g^{\perp}(x)$ is the left annihilator of $g(x)$ which verifies:

$$g^{\perp}(x)g(x) = 0, \tag{20}$$

being

$$\text{rank}(g^{\perp}(x)) = n - m. \tag{21}$$

3) The desired function of power satisfies $(x^*) = \arg\min P_d(x)$. Where the total power function is

$$P_d(x) = P(x) + P_a(x), \tag{22}$$

with

$$P(x) = \int [Q(x)f(x)]^T dx. \tag{23}$$

Under these conditions, the control law is:

$$u = (g^T g)^{-1} g^T \nabla P_a(x). \tag{24}$$

B. Control law

In order to represent the system (12) using the equations of Brayton-Moser, alternative pairs ($Q(x)$, $P(x)$) are proposed, according to [10]. These matrix are presented in the appendix B.

To obtain a function $P_a(x)$, a left annihilator should be proposed and then the partial differential equation (19) be solved. The left annhilator proposed with $rank(g^{\perp}) = n - m = 2$, is

$$g^{\perp}(x) = \begin{bmatrix} 1 & 0 & 0 \\ 0 & 1 & 0 \end{bmatrix}. \tag{25}$$

The partial differential equation, employing the alternative matrix $\tilde{Q}(x)$ and the left annhilator (25) is

$$g^{\perp}\tilde{Q}^{-1}\nabla P_a(x) = \begin{bmatrix} q_{11}\frac{\partial P_a(x)}{\partial x_1} \\ q_{22}\frac{\partial P_a(x)}{\partial x_2} \end{bmatrix} = 0. \tag{26}$$

In the last expression we can observe that $P_a(x)$ no depend of the variables x_1 or x_2. And using the concepts developed by [15], we can propose a function $P_a(x)$ that depends only on the variables x_3 and x_4 respectively. Furthermore, the Lyapunov function $P_d(x) = P(x) + P_a(x)$ must reach a local minimum at the equilibrium point, that is ($\nabla P_d(x^*) = 0$ y $\nabla^2 P_d(x^*) > 0$).

The function $P_a(x)$ was designed considering that the ESS has a finite energy. The ESS just could deliver power when the system is affected by a disturbance in the load or in the wind resource. In this sense we assume that $q_{33}f_3(x^*) = 0$ and also that $q_{44}f_4(x^*) = 0$.

The function $P_a(x)$ proposed is

$$P_a(x) = k_1(x_3 - x_3^*)^2 + k_2(x_4 - x_4^*)^2, \tag{27}$$

being, the Hessian of $P_d(x)$ is positive definite and it is shown in the appendix C.

Then, the control law employing expression (24) is given by

$$u = \begin{bmatrix} -k_{qw}\frac{\partial P_a(x)}{\partial x_3} \\ -k_{pv}T\frac{\partial P_a(x)}{\partial x_4} \end{bmatrix}. \tag{28}$$

C. Sliding mode reference conditioning

In this paper, we consider restrictions on the active and reactive powers that the ESS can deliver. In particular, we apply concepts of sliding mode reference conditioning (SMRC) in order to modify the reference in the control law [16].

For clearly, the loop corresponding to the reactive power has been ommited. The conditioning loop of the ESS active power is shown in Fig. 2. When the system operates within its allowed region $P^- = P_{lim}^- \leq P \leq P_{lim}^+ = P^+$ the signal w is zero and the conditioning loop is not active. This loop acts as follows, when the ESS power exceeds its upper bound, $s = P^+ - P < 0$ and w changes to w^-. Similarly, if P falls below its lower limit w switches to w^+.

From the practical point of view, due to the slow grid dynamic, it is assumed that the switching of w directly affects the first time-derivative of the constrained signal P and the switching function s. Thus, assuming a sufficiently large discontinuous signal w the switching logic assures that:

$$\begin{cases} \dot{s} > 0 & \text{if } s < 0 \\ \dot{s} < 0 & \text{if } s > 0 \end{cases} \tag{29}$$

In this manner, when P intends to surpass one of its limits, w enforces P into its allowed region, where w equals zero again. While the variable P continues trying to cross the system output bound, the signal w will switch between 0 and w_- at high frequency and the system will evolve so that $s = 0$. Consequently, the conditioned signal of reference will be continuously adjusted in such a way that the output P never exceeds the limit.

This signal w, through a LPF, modify the signal of reference achieving the system does not reach saturation [16].

IV. Evaluation of the Control Law

To compare the Lyapunov functions $P(x)$ and $P_d(x)$, we represent in Fig. 3 their contours on the $x_3 - x_4$ plane. We represent the functions $P(x)$ and $P_d(x)$ in dashed line and solid line respectively. The equilibrium point is marked with x^*.

Comparing the labels of the contours in Fig. 3 is noted that $P_d(x)$, with control law, converges faster than $P(x)$, to the equilibrium point. Note that the closed contours belonging to $P_d(x)$ cover a larger neighborhood than corresponding to $P(x)$. Moreover, Opened contours belonging to the function $P(x)$ are shown in the zoom of Fig. 3.

The simulation results are based on the system of the Fig. 1. To evaluate the performance of the controllers, are considered disturbances on active and reactive power at node 1. Also, to verify the SMRC, the active and reactive power that can deliver the ESS was limited. In the first case, we consider a active disturbance in the node 1 depicted in part a of the Fig. 4. In $t = 1.5$ sec, an active power disturbance of 250 kW is detected, which increase to 375 kW in $t = 2.5$ sec. In $t > 5$ sec the active power disturbance disappears. This kind of disturbance could be attributed to a variation in wind generation or a variation in the load.

The second case considered is a variation of reactive power in the load. While in $t = 13$ sec the load consumes 100 kVAr, in $t = 14$ sec the load consumes 200 kVAr and in $t > 18$ sec the reactive power disturbance ceases.

The active and reactive powers of the system are presented in the Figs. 4 and 5, respectively. The contribution of the active and reactive powers of the synchronous generator plus the constant supply of the wind turbine ($(P_w + P_{GS1})$ and $(Q_w + Q_{GS1})$) are shown in the Figures 4b) and 5b). Figs. 4 and 5, parts a, c and d, are shown the powers of the disturbance, static and dynamic loads and finally, the power exchanges by the ESS respectively.

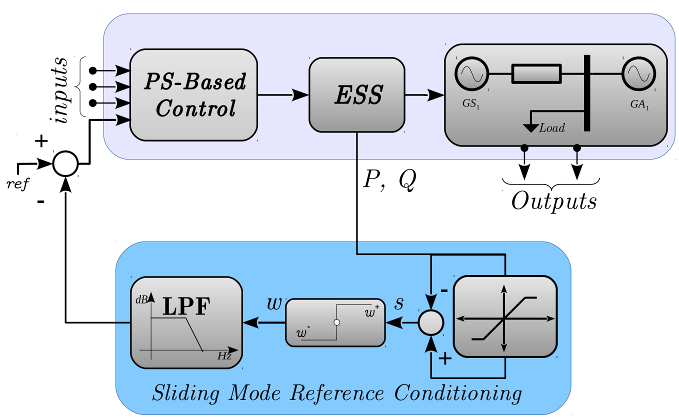

Figure 2. Implementation scheme of SMRC.

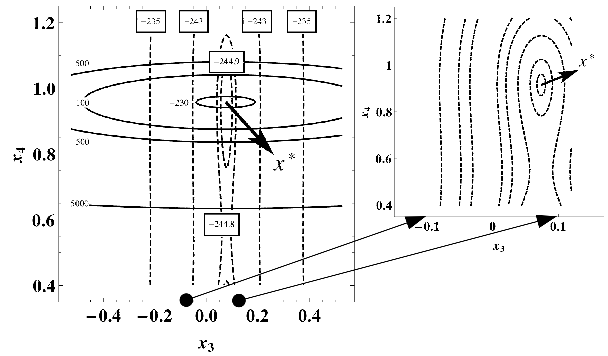

Figure 3. Contours of the $P(x)$ and $P_d(x)$ functions.

In Fig. 6, the voltage (V) and δ in the node 1 are shown.

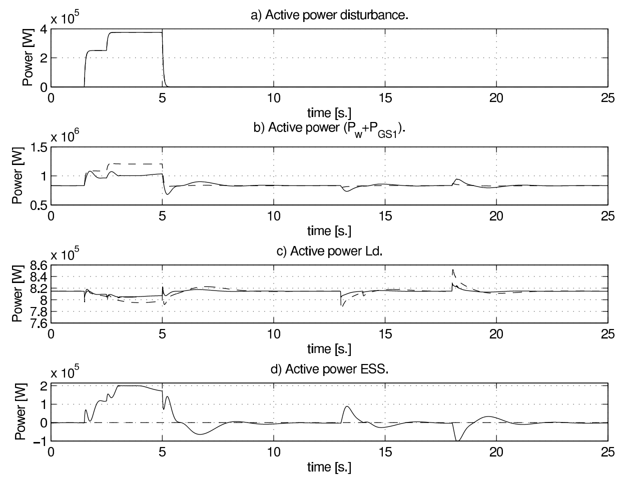

Figure 4. Active power in the electrical grid.

Solid lines correspond to the case when the ESS is used and with dashed lines when it is disconnected.

In the first case considered, in $t > 2.5$ sec, the control loop detects the voltage variation at the node (Fig. 6a)) and the ESS contributes with active power (Fig. 4d)). Later, ESS achieves the maximum power that can deliver and using the SMRC technique, the voltage reference is conditioned to not exceed the maximum power (Fig. 4d)). In addition, in Fig. 4 it can be observed that without the contribution of ESS (dashed line), the synchronous generator has to provide all the power required by the disturbance. The contribution of ESS (solid line) reduce the power supplied by the synchronous generator ($GS1$) (Fig. 4b)).

Also, in Figs. 4c) and 5c) are shown how the dynamic load varies their power consumption due to variations of V and δ in the connection point (Fig. 6).

In the second case considered, (Fig. 5), it is observed that the disturbance in the reactive power causes the variation in the voltage of node 1 and δ (Fig. 6). A variation of δ involves an injection of reactive power by the ESS due to the control law proposed. This injection mitigates the impact of the disturbance of reactive power in δ (Fig. 6b)). Also, a variation in the voltage in the node 1 is observed Fig. 6a). Then, initially ESS produces an injection of active power (Fig. 4d)) and when the voltage rises over the reference voltage, Fig. 6a), the ESS consume active power (Fig. 4d)).

V. Conclusion

In this work, the PS control concepts are used to propose a control law for the active and reactive power that can deliver an ESS. In order to analyze the effects of the restrictions of powers that the ESS can exchange with the electrical grid, a technique based on SMRC was employed for the conditioning of the reference. The scheme proposed in this work could allow better use of the wind resource as well as a reduction in fuel consumption.

One of the advantages of PS-control is the use of knowledge of the structure of the system in the control law interpretation. Moreover, the power shaping ideas facilitate the process to obtain the Lyapunov function which ensures stability in a domain of attraction.

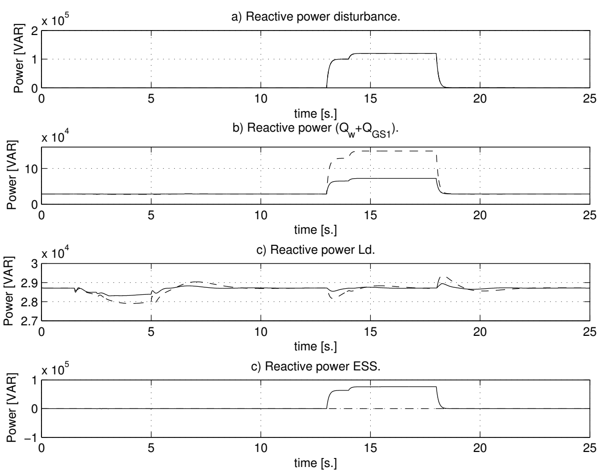

Figure 5. Reactive power.

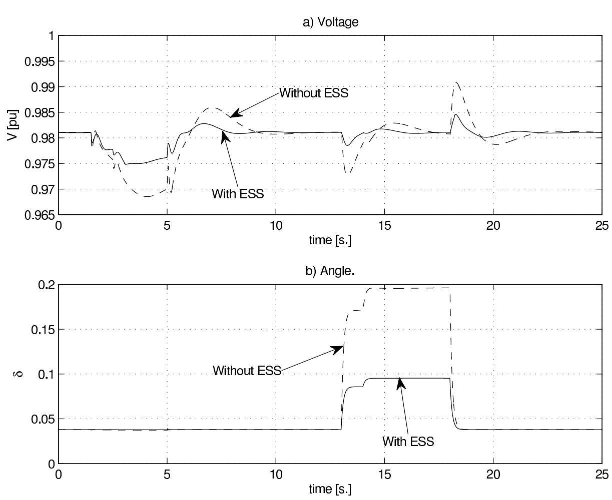

Figure 6. Voltage and δ in node 1.

On the other hand, the control action proposal does not require coordination with other controllers from the mains analyzed.

Appendix A
Load parameters

The values for the parameters of the load are $k_{pw} = 0.4$, $k_{pv} = 0.3$, $T = 8.5$, $k_{qv} = -2.8$, $k_{qv2} = 2.1$, $P_0 = 0$, $P_1 = 0.6$, $Q_0 = 1.3$ and $Q_1 = 0$. All values of the dynamic load are expressed in per unit except the angle which is expressed in degree.

Appendix B
Matrix $\tilde{Q}$

The matrix $Q(x)$ was calculated according to [10; 17], where the authors propose two alternative matrices $Q(x)$ and $P(x)$, denoted as $\tilde{Q}(x)$ and $\tilde{P}(x)$ respectively. The new pair $\tilde{Q}(x)$ and $\tilde{P}(x)$ represent the system given by

$$\tilde{Q}\dot{x} = \nabla\tilde{P} + \tilde{G}u, \tag{30}$$

being

$$\tilde{Q}(x) = \left[\frac{1}{2}\nabla(Qf)M + \frac{1}{2}\nabla^T(MQf) + \lambda I\right] Q, \tag{31}$$

where $\lambda \in \mathbb{R}$ and $M = M^T : \mathbb{R}^n \to \mathbb{R}^{nxn}$, are arbitrary.

The pair $\tilde{P}(x)$ is given by

$$\tilde{P}(x) = \lambda \int (Qf)^T dx + \frac{1}{2} f^T Q^T M Q f, \tag{32}$$

and

$$\tilde{G} = \tilde{Q}g. \tag{33}$$

The matrices M and Q proposed determines the symmetrical structure of the matrix $\tilde{Q}$. This choice together with the left annihilator $g^{\perp}(x)$ gives us a way for PDE. The solution of the PDE allows us to design a function $P_a(x)$.

$$M = 0_4, \tag{34}$$

$$Q(x) = I_4, \tag{35}$$

being I_4 a identity matrix of 4x4 and O_4 a zero matrix of 4x4.

$$\lambda = \lambda_1 I_4, \tag{36}$$

where $\lambda_1 = -1$, then the matrix $\tilde{Q}(x)$ is

$$\tilde{Q}(x) = -1 I_4, \tag{37}$$

and at the same time $\tilde{Q}(x)$ accomplish with the condition (17) and (18).

Appendix C
Hessian

To verify that $P_d(x)$ is a candidate Lyapunov function, Hessian is positive definite in the equilibrium point. The Hessian is given by

$$\nabla^2 P_d(x) = \begin{pmatrix} \frac{D_i}{M_i} & 0 & 0 & 0 \\ 0 & \frac{1}{T_A} & 0 & 0 \\ 0 & 0 & 2k_1 & 0 \\ 0 & 0 & 0 & 2k_2 \end{pmatrix} > 0. \quad (38)$$

The condition ($\nabla^2 P_d(x^*) > 0$) can be verified by checking that the principal minors of the matrix (38) are positive and adjusting the values of the constant k_1 and k_2.

Acknowledgment

This work has been performed through CONICET, UNPSJB, UNLP, CICpBA.

References

[1] H. Nikkhajoei and R. Lasseter, "Distributed generation interface to the certs microgrid," *Power Delivery, IEEE Transactions on*, vol. 24, no. 3, pp. 1598–1608, July 2009.

[2] M. Cheng and Y. Zhu, "The state of the art of wind energy conversion systems and technologies: A review," *Energy Conversion and Management*, vol. 88, pp. 332 – 347, 2014.

[3] M. Chowdhury, M. Haque, M. Aktarujjaman, M. Negnevitsky, and A. Gargoom, "Grid integration impacts and energy storage systems for wind energy applications - a review," in *Power and Energy Society General Meeting, 2011 IEEE*, July 2011, pp. 1–8.

[4] F. D. Bianchi, H. De Battista, and R. J. Mantz, *Wind turbine control systems: Principles, modelling and gain scheduling design*, ser. Advances in Industrial Control series. London: Springer-Verlag London Ltd., 2006.

[5] V. Boicea, "Energy storage technologies: The past and the present," *Proceedings of the IEEE*, vol. 102, no. 11, pp. 1777–1794, Nov 2014.

[6] X. Tang, W. Deng, and Z. Qi, "Research on microgrid voltage stability control based on supercapacitor energy storage," in *Electrical Machines and Systems, 2009. ICEMS 2009. International Conference on*, Nov 2009, pp. 1–6.

[7] ——, "Investigation of the dynamic stability of microgrid," *Power Systems, IEEE Transactions on*, vol. 29, no. 2, pp. 698–706, March 2014.

[8] R. Ortega, D. Jeltsema, and J. M. A. Scherpen, "Power shaping: a new paradigm for stabilization of nonlinear rlc circuits," *Automatic Control, IEEE Transactions on*, vol. 48, no. 10, pp. 1762–1767, 2003.

[9] E. García-Canseco, D. Jeltsema, R. Ortega, and J. M. Scherpen, "Power-based control of physical systems," *Automatica*, vol. 46, no. 1, pp. 127 – 132, 2010.

[10] E. Garcia-Canseco, R. Ortega, J. M. A. Scherpen, and D. Jeltsema, "Power shaping control of nonlinear systems: A benchmark example." *Lecture notes in control and Information sciences*, no. 366, pp. 135 – 146, 2007.

[11] P. Sauer, *Power system dynamics and stability*. Upper Saddle River, N.J: Prentice Hall, 1998.

[12] P. Kundur, *Power system stability and control*. New York: McGraw-Hill, 1994.

[13] P. M. Anderson, *Power system control and stability*. Piscataway, N.J: IEEE Press, 1994.

[14] I. Dobson and H.-D. Chiang, "Towards a theory of voltage collapse in electric power systems," *Systems & Control Letters*, vol. 13, no. 3, pp. 253 – 262, 1989.

[15] M. Galaz, R. Ortega, A. S. Bazanella, and A. M. Stankovic, "An energy-shaping approach to the design of excitation control of synchronous generators," *Automatica*, vol. 39, no. 1, pp. 111 – 119, 2003.

[16] F. Garelli, R. J. Mantz, and H. D. Battista, *Advanced control for constrained processes and systems*. Stevenage: Institution of Engineering and Technology, 2011.

[17] D. Jeltsema, *Modeling and Control of Nonlinear Networks: A Power-Based Perspective*. Delft University of Technology, 2005.